Journal of Zhejiang University-SCIENCE B (Biomedicine & Biotechnology)
ISSN 1673-1581 (Print); ISSN 1862-1783 (Online)
www.zju.edu.cn/jzus; www.springerlink.com
E-mail: jzus@zju.edu.cn

In vitro remineralization of hybrid layers using biomimetic analogs*

Hui-ping LIN[1], Jun LIN[†‡1], Juan LI[1], Jing-hong XU[1], Christian MEHL[†‡2]

([1]*Department of Stomatology, the First Affiliated Hospital, School of Medicine, Zhejiang University, Hangzhou 310003, China*)

([2]*HarderMehl Dental Clinic, Volkartstraße 5, 80634 Munich, Germany*)

[†]E-mail: junlin2@126.com; cmehl@proth.uni-kiel.de

Received Apr. 5, 2016; Revision accepted June 23, 2016; Crosschecked Oct. 18, 2016

Abstract: Resin-dentin bond degradation is a major cause of restoration failures. The major aim of the current study was to evaluate the impact of a remineralization medium on collagen matrices of hybrid layers of three different adhesive resins using nanotechnology methods. Coronal dentin surfaces were prepared from freshly extracted premolars and bonded to composite resin using three adhesive resins (FluoroBond II, Xeno-III-Bond, and iBond). From each tooth, two central slabs were selected for the study. The slabs used as controls were immersed in a simulated body fluid (SBF). The experimental slabs were immersed in a Portland cement-based remineralization medium that contained two biomimetic analogs (biomineralization medium (BRM)). Eight slabs per group were retrieved after 1, 2, 3, and 4 months, respectively and immersed in Rhodamine B for 24 h. Confocal laser scanning microscopy was used to evaluate the permeability of hybrid layers to Rhodamine B. Data were analyzed by analysis of variance (ANOVA) and Tukey's honest significant difference (HSD) tests. After four months, all BRM specimens exhibited a significantly smaller fluorescent area than SBF specimens, indicating a remineralization of the hybrid layer ($P \leq 0.05$). A clinically applicable biomimetic remineralization delivery system could potentially slow down bond degradation.

Key words: Remineralization, Dentin, Adhesive resin, Biomimetic analog, Altered collagen, Confocal laser scanning microscopy (CLSM), Fluorescence

http://dx.doi.org/10.1631/jzus.B1600151 **CLC number:** R783.1

1 Introduction

The stability of the hybrid layer is inadvertently compromised during the bonding of resin and dentin. Firstly, etching and rinsing can degenerate the denuded collagen fibrils within the hybrid layer (Carrilho *et al.*, 2007). Secondly, demineralized collagen fibrils may collapse via inter-peptide hydrogen bonding when they are air-dried during bonding, restricting the infiltration of adhesive resin monomers (Pashley *et al.*, 2007; Mai *et al.*, 2009). Thirdly, due to fluid movement within the dentinal tubules during resin infiltration, often aggravated by the presence of a positive pulpal pressure, monomers only inadequately infiltrate the dentin (Wang and Spencer, 2005; Hashimoto, 2010; Lin *et al.*, 2010). These procedural obstacles accelerate in vivo degradation of hybrid layers (Kim J. *et al.*, 2010). Degradation occurs as early as six months after initial intraoral function (Kim J. *et al.*, 2010). It is triggered by hydrolysis of suboptimally polymerized hydrophilic resin components and degradation of water-rich, resin-sparse collagen matrices by matrix metalloproteinases and cysteine cathepsins (Tjaderhane *et al.*, 1998; Pashley *et al.*, 2004; Liu *et al.*, 2011). Subsequently, the compromised hybrid layer causes leakage in the nano-space of the collagen fibers, leading to restoration failure (Li *et al.*, 2000).

Several strategies have been developed to stabilize the bond between composite resin and dentin and thus prevent restoration failure (Liu *et al.*, 2011).

‡ Corresponding authors

* Project supported by the National Natural Science Foundation of China (No. 81271955) and the Zhejiang Provincial Natural Science Foundation of China (No. Y2080338)

ORCID: Christian MEHL, http://orcid.org/0000-0001-7541-1021

Biomimetic remineralization is a recent approach using analogs of matrix proteins to progressively replace water with intrafibrillar and extrafibrillar apatites in order to exclude exogenous collagenolytic enzymes and fossilize endogenous collagenolytic enzymes (Zhang, 2003; Tay *et al.*, 2007; Tay and Pashley, 2008).

Most biomimetic remineralization studies have used transmission electron microscopy to evaluate the interface between adhesive and resin and the degree of remineralization (Kinney *et al.*, 2003; Carrilho *et al.*, 2005; Trebacz and Wojtowicz, 2005; Tay and Pashley, 2009; Gu *et al.*, 2010; Kim Y.K. *et al.*, 2010b). Confocal laser scanning microscopy (CLSM) using Rhodamine B uptake by demineralized or incompletely resin-infiltrated collagen fibers seems to be a promising new method to evaluate remineralization effects (Kim J. *et al.*, 2010). Hence, the current study aimed to use CLSM to evaluate three commercial representative bonding adhesive resins based on three different working mechanisms.

The null-hypotheses with regard to Rhodamine B uptake of the hybrid layers to be tested were: (1) there is no difference between a two-step etch-and-rinse adhesive resin, a self-etching one-step two-bottle adhesive resin, and a self-etching one-bottle adhesive resin; (2) the placement of the experimental specimens in a remineralization medium has no effect in comparison to a control group; and, (3) the duration of immersion has no effect.

2 Materials and methods

2.1 Tooth preparation

Ninety-six intact human premolars were extracted and stored in 0.5% (5 g/L) thymol-saturated isotonic saline solution at 4 °C. The teeth were collected after the patients' informed consents were obtained under a protocol approved by the Ethics Committee of the Faculty of Dentistry at the Zhejiang University, China. All teeth were used within three months after extraction. A flow chart of the experimental process can be found in Fig. 1.

The occlusal enamel was removed perpendicular to the longitudinal axis of each tooth using a slow-speed diamond saw (Isomet, Buehler, Lake Bluff, IL, USA) under water cooling (Lin *et al.*, 2014). The resulting flat dentin surface was checked with a stereomicroscope (Wild Makroskop M420, Heerbrugg, Switzerland) at 10× magnification for the absence of enamel (Lin *et al.*, 2014). The dentin bonding surfaces were polished with a 600-grit silicon carbide paper (Buehler) to create a standardized smear layer in mid-coronal dentin (MP-260E, Weiyi Instrument Test Equipment Manufacturing, Laizhou City, China) (Yang *et al.*, 2006). For all specimens, the dentin was kept wet during all preparations by storage in deionized water or placement on a wet dish.

2.2 Tooth conditioning and bonding procedures

The composition of the main materials used in this study can be found in Table 1. The three adhesive resins were chosen as representatives of commercially available bonding adhesive resins with different bonding methodologies. A two-step etch-and-rinse adhesive resin (FluoroBond II, Shofu, Japan), and two one-step adhesive resins (Xeno-III-Bond, Dentsply, York, PA, USA and iBond, Heraeus, Hanau, Germany) were used according to the manufacturers' instructions. Following the adhesive procedures, a composite resin filling material was built up incrementally to a height of 5 mm (Valux Plus Restorative, 3M Espe, St. Paul, MN, USA). Each layer was light-cured separately for 20 s (output intensity 1500 mW/cm^2; Satelec, Bordeaux, France). Each tooth was sectioned occluso-gingivally. Only the two central 0.9 mm thick slabs were used. Overall, 24 experimental groups with 8 specimens were tested (3 adhesive resins, storage for 1, 2, 3, or 4 months and control group/experimental group; Fig. 1). Before experimentation, all specimens were stored in deionized water at room temperature and used within 24 h.

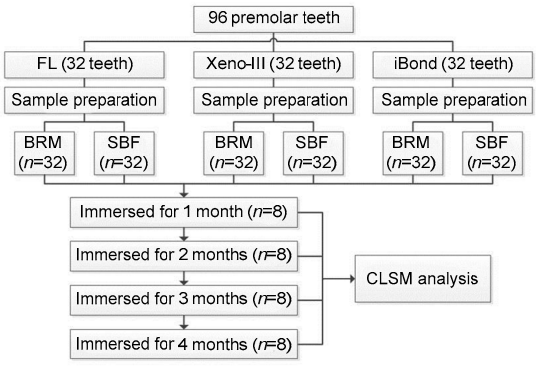

Fig. 1 Experimental set-up used in this study
FL: FluoroBond II; BRM: biomineralization medium; SBF: simulated body fluid; CLSM: confocal laser scanning microscopy

Table 1 Composition of the three adhesive resins used in this study

Name	Etching/steps	Company & batch No.	Principal component
FluoroBond II	Two-step	Shofu, Kyoto, Japan; 0609	Primer: ethanol, carboxylic acid monomer, phosphoric acid monomer and initiator, water; Bonding agent: S-PRG filler on fluoroboroaluminosilicate glass, UDMA, TEGDMA, 2-HEMA, initiator
Xeno-III-Bond	One-step (mixed)	Dentsply, York, PA, USA; 0909001714	Liquid A: HEMA, ethanol, BHT, 2,6-di-*tert*-butyl-*p*-hydroxytoluol, water, nanofillers; Liquid B: pyro-EMA, PEM-F, BHT, camphorquinone, *p*-dimethylamino-ethyl-benzoat
iBond	One-step (not mixed)	Heraeus, Hanau, Germany; 010102	An acetone/water-based formulation of light-activated methylacrylate resins

S-PRG: surface pre-reacted glass-ionomer; UDMA: urethane dimethacrylate; TEGDMA: triethylene-glycol-dimethacrylate; HEMA: hydroxyethyl-methacrylate; BHT: butylated hydroxy toluidine; Pyro-EMA: tetramethacryloxyethyl pyrophosphate; PEM-F: pentamethacryloxyethyl cyclophosphazen mono fluoride

2.3 Biomimetic remineralization procedures and control group preparation

For the control group, simulated body fluid (SBF) solution was prepared by dissolving 136.8 mmol/L NaCl, 4.2 mmol/L $NaHCO_3$, 3.0 mmol/L KCl, 1.0 mmol/L $K_2HPO_4{\cdot}3H_2O$, 1.5 mmol/L $MgCl_2{\cdot}6H_2O$, 2.5 mmol/L $CaCl_2$, and 0.5 mmol/L Na_2SO_4 in deionized water (Kokubo *et al.*, 1990), and adding 3.08 mmol/L sodium azide to stop bacteria from growing. Tris base at 0.1 mol/L and HCl at 0.1 mol/L were used to buffer the SBF to a pH value of 7.4 and the resulting solution was filtered (Kim J. *et al.*, 2010).

For the experimental groups, initially a Portland cement block was prepared. For that purpose, deionized water was mixed with Type I white Portland cement (Lehigh Cement Company, Allentown, PA, USA) in a water-to-powder ratio of 0.35:1 (w/w). Before it was used for this study, the resulting solution was filtered and stored at 100% relative humidity for one week in silicone molds (Tay *et al.*, 2007; Mai *et al.*, 2009; Sauro *et al.*, 2015). The experimental slabs were then placed on the established blocks of Portland cement (ca. 1 g) inside a glass cylinder (Mai *et al.*, 2009; Kim J. *et al.*, 2010). The biomineralization medium (BRM) was produced by adding 500 μg/ml of polyacrylic acid (PAA; molecular weight (MW) 1800; Sigma-Aldrich, St. Louis, MO, USA) and 200 μg/ml of polyvinylphosphonic acid (PVPA; MW 10177; Sigma-Aldrich) to the SBF. The solution was buffered again to a pH of 7.4 (Mai *et al.*, 2009; Kim J. *et al.*, 2010).

The glass cylinders containing the slabs were either filled with 15 ml of the SBF (control group) or BRM (experimental group), and stored at 37 °C (Mai *et al.*, 2009; Kim J. *et al.*, 2010).

The remineralization medium was changed every month (Kim J. *et al.*, 2010). To ensure that apatite was formed instead of octacalcium phosphate (Meyer and Weatherall, 1982; Eanes, 2001), the pH (after placing on the Portland cement blocks) was monitored weekly and adjusted if necessary to maintain it above 9.25 (Mai *et al.*, 2009; Kim J. *et al.*, 2010).

After 1, 2, 3, and 4 months, respectively, eight slabs for each adhesive resin were retrieved and immersed in a 0.1 mmol/L Rhodamine B solution (CAS81-88-9, MW 479, Shanghai Chemicals, China). After 24 h, the dye-infiltrated slabs were rinsed with deionized water for 30 s and examined using a CLSM that was coupled with a helium neon gas laser (Laser Scanning Confocal Microscope TCS-SP2, Leica, Wetzlar, Germany; 50% of 543 nm excitation, 383 V, and magnification of 40×4). Images were captured starting from 10 μm beneath the surface to avoid superficial specimen preparation artifacts. The total fluorescent area, average fluorescence (AF), and total fluorescence (TF) were measured using Image-Pro-Plus 6.0 software in the region of interest (ROI). The ROI was defined as the region between the composite and the dentin, including the hybrid layer and adhesive resin layer. The fluorescent area was the area of mineral deficiency in the hybrid layers (Sidhu and Watson, 1998; Watson *et al.*, 2008); the AF represented the fluorescence intensity of the defect area in the hybrid layers; and the TF represented the sum of all fluorescent pixels in the mineral defect area.

2.4 Statistical analysis

The data were analyzed using a statistical software package (SPSS 18.0, Chicago, IL, USA). Since

data were distributed normally (Shapiro-Wilks and Kolmogorov-Smirnov tests), parametric tests were employed (three-way analysis of variance (ANOVA) (least significant difference (LSD)) and Tukey's honest significant difference (HSD) tests). All testing was performed at a confidence level of 95%.

3 Results

Three-way ANOVA results are presented in Table 2. For each adhesive resin, the fluorescent area, AF, and TF are presented in Tables 3–5. The choice of adhesive resin, the use of a remineralizing medium

Table 2 Three-way ANOVA of the data to evaluate the influences of the adhesive resins, the remineralizing medium, and the immersion time on fluorescent area, average fluorescence (AF), and total fluorescence (TF)

Source	Area		AF		TF	
	F value	*P* value	*F* value	*P* value	*F* value	*P* value
Adhesive resins	212.490	0.000	0.620	0.539	192.587	0.000
FluoroBond II						
Xeno-III-Bond						
iBond						
Remineralizing medium	20.510	0.000	0.077	0.782	13.591	0.000
SBF						
BRM						
Immersed time	2.674	0.049	11.819	0.000	3.443	0.018
First month						
Second month						
Third month						
Forth month						

Table 3 Confocal laser scanning microscopy (CLSM) analysis using Image-Pro-Plus 6.0 software to measure the fluorescent area, average fluorescence (AF), and total fluorescence (TF) for FluoroBond II

Immersed time (month)	Area (μm^2)		AF ($\times 10^{-3}$)		TF (μm^2)	
	SBF	BRM	SBF	BRM	SBF	BRM
1	$2232.2\ (501.2)^{a}{}_{A}$	$2060.4\ (226.2)^{a}{}_{A}$	$113.2\ (5.5)^{a}{}_{A}$	$109.6\ (7.5)^{a}{}_{A}$	$302.5\ (71.6)^{a}{}_{A}$	$281.0\ (42.7)^{a}{}_{A}$
2	$1914.7\ (252.6)^{a}{}_{A}$	$1974.8\ (582.2)^{a,b}{}_{A}$	$100.8\ (12.3)^{b}{}_{A}$	$98.9\ (9.5)^{b}{}_{A}$	$232.1\ (27.8)^{b}{}_{A}$	$236.7\ (78.4)^{a,b}{}_{A}$
3	$2240.0\ (384.4)^{a}{}_{A}$	$1953.2\ (497.6)^{a,b}{}_{A}$	$108.8\ (8.5)^{b}{}_{A}$	$110.7\ (6.0)^{a,b}{}_{A}$	$284.6\ (52.9)^{a,b}{}_{A}$	$263.7\ (70.7)^{a,b}{}_{A}$
4	$2162.4\ (564.2)^{a}{}_{A}$	$1573.3\ (435.4)^{b}{}_{B}$	$108.1\ (12.9)^{b}{}_{A}$	$110.8\ (9.1)^{a}{}_{A}$	$268.2\ (67.7)^{a,b}{}_{A}$	$218.1\ (67.3)^{b}{}_{A}$

All data are expressed as mean (SD), n=8. The same superscript lowercase letters indicate no statistical significance between the different immersion times of the adhesive resins for each experimental group (P>0.05). The same subscript uppercase letters indicate no statistical significance between SBF and BRM for each immersion time (P>0.05)

Table 4 Confocal laser scanning microscopy (CLSM) analysis using Image-Pro-Plus 6.0 software to measure the fluorescent area, average fluorescence (AF), and total fluorescence (TF) for Xeno-III-Bond

Immersed time (month)	Area (μm^2)		AF ($\times 10^{-3}$)		TF (μm^2)	
	SBF	BRM	SBF	BRM	SBF	BRM
1	$555.7\ (101.3)^{a}{}_{A}$	$630.9\ (132.4)^{a}{}_{A}$	$102.1\ (11.7)^{a}{}_{A}$	$118.5\ (14.5)^{a}{}_{B}$	$66.4\ (11.5)^{a}{}_{A}$	$82.6\ (17.8)^{a}{}_{B}$
2	$924.0\ (225.6)^{b}{}_{A}$	$664.0\ (233.0)^{a,b}{}_{B}$	$104.4\ (11.0)^{a}{}_{A}$	$100.2\ (5.5)^{b}{}_{A}$	$118.1\ (30.8)^{b}{}_{A}$	$80.2\ (29.9)^{a,b}{}_{B}$
3	$889.6\ (84.0)^{b}{}_{A}$	$479.2\ (69.7)^{b}{}_{B}$	$106.1\ (13.7)^{a}{}_{A}$	$108.8\ (11.8)^{a,b}{}_{A}$	$113.4\ (37.9)^{b}{}_{A}$	$59.2\ (11.7)^{b}{}_{B}$
4	$989.6\ (141.8)^{b}{}_{A}$	$517.7\ (114.2)^{a,b}{}_{B}$	$109.7\ (8.1)^{a}{}_{A}$	$117.6\ (11.4)^{a}{}_{A}$	$121.6\ (17.7)^{b}{}_{A}$	$69.7\ (17.4)^{a}{}_{B}$

All data are expressed as mean (SD), n=8. The same superscript lowercase letters indicate no statistical significance between the different immersion times of the adhesive resins for each experimental group (P>0.05). The same subscript uppercase letters indicate no statistical significance between SBF and BRM for each immersion time (P>0.05)

Table 5 Confocal laser scanning microscopy (CLSM) analysis using Image-Pro-Plus 6.0 software measuring the fluorescent area, average fluorescence (AF), and total fluorescence (TF) for iBond

Immersed time (month)	Area (μm^2)		AF ($\times10^{-3}$)		TF (μm^2)	
	SBF	BRM	SBF	BRM	SBF	BRM
1	2640.1 (876.5)$^{a}_{A}$	2321.7 (819.3)$^{a}_{A}$	105.5 (3.8)$^{a}_{A}$	102.3 (10.3)$^{a}_{A}$	355.0 (126.3)$^{a,b}_{A}$	294.9 (111.9)$^{a}_{A}$
2	2308.9 (234.3)$^{a}_{A}$	1921.3 (267.9)$^{a,b}_{B}$	97.9 (9.2)$^{b}_{A}$	101.0 (8.5)$^{a}_{A}$	283.9 (43.0)$^{a,b}_{A}$	240.9 (32.5)$^{a}_{B}$
3	1980.9 (578.1)$^{a}_{A}$	1571.1 (465.4)$^{b}_{A}$	116.7 (10.6)$^{c}_{A}$	110.5 (8.5)$^{a}_{A}$	257.4 (71.4)$^{a}_{A}$	212.7 (67.0)$^{a}_{A}$
4	2549.6 (466.5)$^{a}_{A}$	1984.4 (553.1)$^{a,b}_{B}$	114.3 (11.9)$^{a,c}_{A}$	107.3 (4.7)$^{a}_{A}$	333.0 (78.1)$^{b}_{A}$	268.6 (72.0)$^{a}_{A}$

All data are expressed as mean (SD), n=8. The same superscript lowercase letters indicate no statistical significance between the different immersion times of the adhesive resins for each experimental group (P>0.05). The same subscript uppercase letters indicate no statistical significance between SBF and BRM for each immersion time (P>0.05)

(SBF vs. BRM), and the duration of immersion had a significant impact on the fluorescent area and TF (P≤0.05). For the AF, only the duration of immersion was significantly influential (P≤0.05).

iBond specimens and FluoroBond II specimens showed the largest fluorescent area (P>0.05), followed by Xeno-III-Bond with a significantly lower fluorescent area (P≤0.05). With the exception of Xeno-III-Bond specimens after one month and FluoroBond II specimens after two months, all BRM groups showed a lower Rhodamine B uptake than the SBF groups (fluorescent area, Fig. 2). For FluoroBond II and iBond, no statistical differences could be found for SBF groups among the different storage times (P>0.05). In contrast, using Xeno-III-Bond, the fluorescent area was significantly larger after 2, 3, and 4 months than after 1 month (P=0.002). Most importantly, a statistical significant difference could be found for all adhesive resins when comparing the SBF and BRM groups at the 4th month (P≤0.05). This finding was supported by CLSM images (Figs. 3–5), in which Rhodamine B uptake was visually equal for all SBF specimens, while BRM specimens at the 4th month showed less Rhodamine B infiltration and stabilization of the dentinal collagen fiber network.

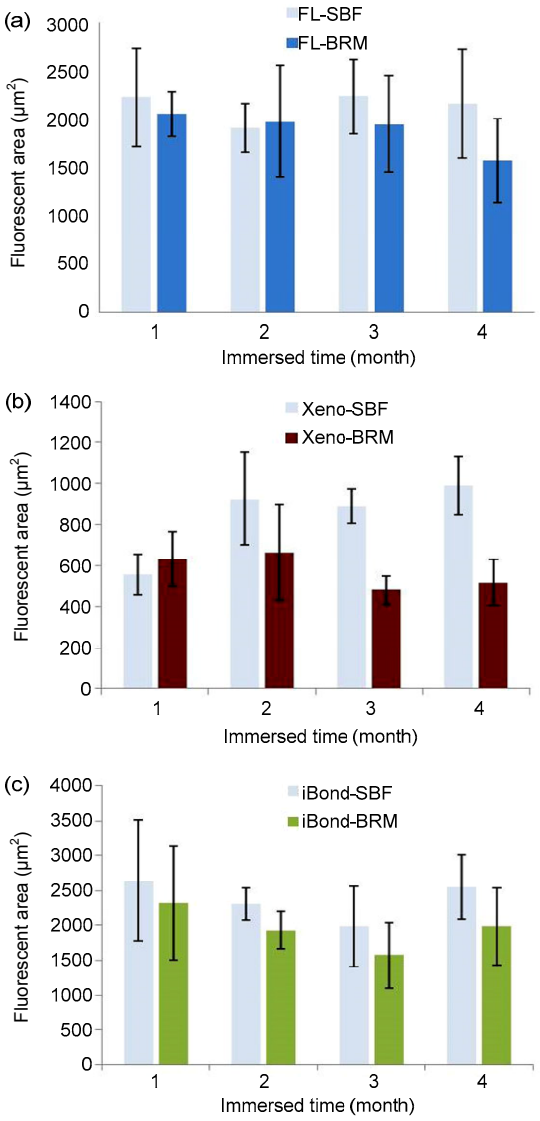

Fig. 2 Relationship between fluorescent area in the hybrid layer and infiltration time for FluoroBond II (a), Xeno-III-Bond (b), and iBond (c) in SBF and BRM
All data are expressed as mean±SD, with n=8

4 Discussion

The null hypotheses could not be accepted, as the factors adhesive resin, remineralization medium, and duration of immersion were each found to have significant effects on Rhodamine B uptake of the hybrid layer.

Because collagen fibers are reinforced with minerals, healthy dentin can provide the tooth with

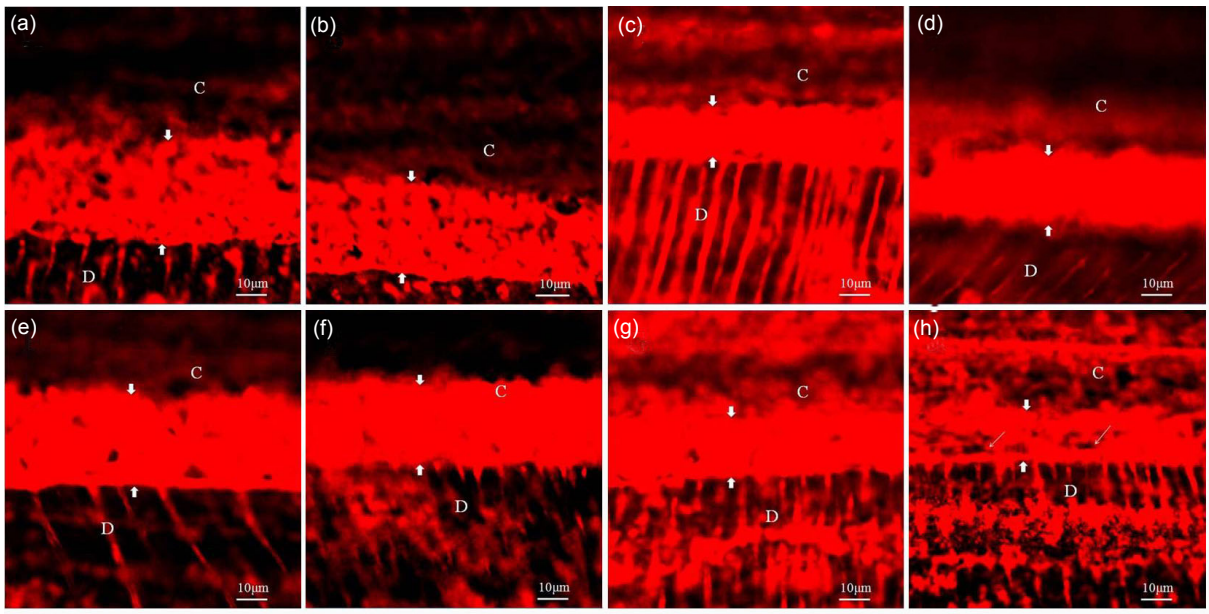

Fig. 3 Representative confocal laser scanning microscopy (CLSM) images (magnification 160×) obtained from one to four months old FluoroBond II specimens

C: composite; D: dentin. (a) The CLSM image of a specimen immersed in SBF for one month shows that most of the hybrid layer (between short arrows, the same below) and the superficial dentinal tubules were permeable to Rhodamine B, but not the mineralized peritubular dentin; (b) The CLSM image of a specimen immersed in BRM for one month shows that the hybrid layer was permeable to Rhodamine B, with no significant difference from that of (a); (c) The CLSM image of a specimen immersed in SBF for two months shows uniform Rhodamine B uptake throughout the hybrid layer and the dentinal tubules; (d) The CLSM image of a specimen immersed in BRM for two months shows the same fluorescence stripe as in (c), just slightly wider; (e) Three-month CLSM image of a specimen immersed in SBF shows a 25-μm thick hybrid layer infiltrated with Rhodamine B; (f) Three-month CLSM image of a specimen immersed in BRM exhibits a 25-μm thick red fluorescent stripe, with no significant difference from that of (e); (g) Four-month CLSM image of a specimen immersed in SBF shows no difference from that of (a), (c), and (e); (h) Four-month CLSM image of a specimen immersed in BRM displays areas of remineralization in the hybrid layer (long thin arrows), which could indicate mineral re-deposition

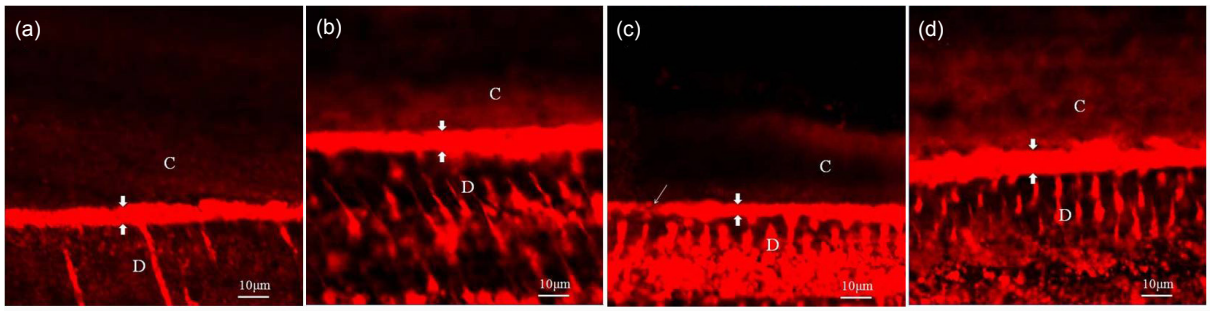

Fig. 4 Representative confocal laser scanning microscopy (CLSM) images (magnification 160×) obtained from one and three months old Xeno-III-Bond specimens

C: composite; D: dentin. (a) One-month CLSM image of specimens immersed in SBF shows that the entire hybrid layer (between short arrows, the same below) was permeated by Rhodamine B; (b) One-month CLSM image of specimens immersed in BRM exhibits no difference from that of (a); (c) Three-month CLSM image of specimens immersed in BRM exhibits a solidly permeated hybrid layer and tubular dentin (long thin arrows); (d) Three-month CLSM image of specimens immersed in SBF shows the entire hybrid layer infiltrated with Rhodamine B, but the tubular dentin mainly left unpermeated

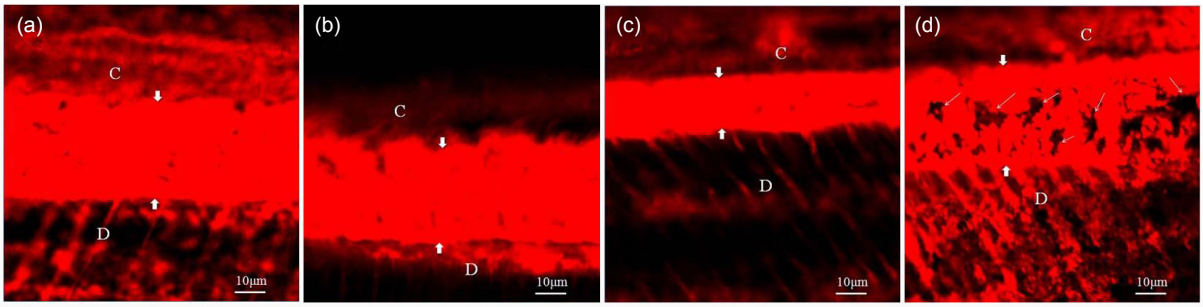

Fig. 5 Representative confocal laser scanning microscopy (CLSM) images (magnification 160×) obtained from one and three months old iBond specimens

C: composite; D: dentin. (a) One-month CLSM image of a specimen immersed in SBF shows that the entire hybrid layer (between short arrows, the same below) of about 30 μm thickness was completely permeable to Rhodamine B; (b) One-month CLSM image of a specimen immersed in BRM exhibits no difference from that of (a); (c) Three-month CLSM image of a specimen immersed in SBF shows that the entire hybrid layer of about 20 μm thickness was infiltrated by Rhodamine B; (d) Three-month CLSM image of a specimen immersed in BRM shows zones of reduced fluorescence in irregularly shaped and varied sizes (long thin arrows)

very good strength and toughness (Kinney *et al.*, 2003; Mai *et al.*, 2009). To be incorporated into the gap zones of the collagen fibers, these minerals need to be sufficiently small and be arranged in a specific way (Xu *et al.*, 2007; Mai *et al.*, 2009).

Collagen fibers are first formed during the mineralization of biological hard tissues, in which water from the intrafibrillar compartments is replaced by apatites (Glimcher, 2006). This process is dependent on the modulation of type I collagen fibers for growth of crystals, in which apatite crystals, assembled by type I collagen fibers, and hydroxyapatite are arranged along the long axis within the mineralized collagen fibers (Glimcher, 2006). The passage of molecules is dramatically reduced when demineralized dentin collagen is replaced by apatite minerals (Glimcher, 2006). Water-soluble molecules below a molecular mass of 6 kDa can diffuse into the water compartments of a collagen fiber, while those greater than 40 kDa cannot (Toroian *et al.*, 2007). As the channels become narrower during mineralization, the speed and volume of water-soluble molecules diffusing through mineralized collagen matrix decrease (Toroian *et al.*, 2007). With a molecular mass of 0.479 kDa, Rhodamine B molecules easily diffuse into the demineralized or incompletely resin-infiltrated collagen fibers. After three months, the amount of Rhodamine B molecules penetrating the resin-sparse regions of the hybrid layer was reduced for all adhesive resins immersed in remineralizing solution, indicating mineral deposition in the collagen matrices. In contrast, Rhodamine B uptake from specimens immersed in SBF remained almost constant.

Compared to transmission electron microscopy, CLSM requires no preparation of thin specimens and is therefore simple and fast (Fontana *et al.*, 1996; Pfarrer *et al.*, 1996; Zhong *et al.*, 2015). When using CLSM, the intensity of a fluorescent dye penetrating an artificial carious dentin lesion is proportional to the porosity or loss of mineral density within the lesion (van der Veen *et al.*, 1996; Jardine *et al.*, 2016). For this reason, re- or demineralization can be quantitatively measured by the fluorescence area, TF, and AF (Fontana *et al.*, 1996; Jardine *et al.*, 2016).

The Portland cement-based remineralization protocol introduced in 2008 uses biomimetic analogs to guide apatite remineralization (Tay *et al.*, 2007; Tay and Pashley, 2008). According to this approach, a PAA with a low MW is used to imitate the stabilizing function of dentin matrix protein 1 (DMP1) on amorphous calcium phosphate precursors (He *et al.*, 2005; Mai *et al.*, 2009; Zhong *et al.*, 2015). The interaction of the Portland cement with SBF reduces these precursors to a nanoscale (Olszta *et al.*, 2003; Mai *et al.*, 2009) and thus prevents their aggregation and precipitation (Cai and Tang, 2008; Mai *et al.*, 2009; Zhong *et al.*, 2015). PVPA, the other biomimetic analog, is a polyanion that imitates the negative charges of phosphoproteins (e.g. DMP1), phosphophoryn, or bone sialoprotein and their roles in organizing parts of the mineralization process (Gajjeraman *et al.*, 2007; Baht *et al.*, 2008; Mai *et al.*, 2009). In our

study, Figs. 3h, 4d, and 5d and the quantitative analysis from specimens immersed in BRM show reduced fluorescence zones, suggesting mineral re-deposition, in agreement with the literature (Kim J. *et al.*, 2010; Kim Y.K. *et al.*, 2010a; Zhong *et al.*, 2015).

Some fluoride-releasing adhesive resins may induce crystal growth within fluid-filled gaps of resin-dentin interfaces without biomimetic remineralization (Hashimoto *et al.*, 2008). However, note that in the current study apatite deposition occurred using non-fluoride-releasing adhesive resins in the absence of interfacial gaps. The remineralization effect of iBond was most obvious and had the fastest emergence time. Most of the remineralization with iBond occurred between one and three months and did not improve further after four months. This finding is similar to an apparent self-limitation of remineralization in primary dentin observed by Kim J. *et al.* (2010) using Adper Prompt L-Pop, a one-step self-etch adhesive resin. The remineralization effect on specimens bonded with Xeno-III-Bond was not as obvious as for iBond. In FluoroBond II, one-month-old specimens, Rhodamine B-free areas could be found in the hybrid layer for specimens immersed in SBF and BRM alike (Figs. 3a and 3b). These areas were significantly reduced in two- and three-month-old specimens (Figs. 3c–3f), while for the four-month-old specimens immersed in SBF the fluorescence of the hybrid layer remained unchanged. BRM specimens showed less Rhodamine B uptake, indicating a possible remineralization.

Rhodamine B uptake was reduced for all adhesive resins tested in the current study when placed in the biomineralizing medium, which is a promising result. However, no solution-based systems can yet be used clinically and basic science may here only pave the way for the development of future usable techniques (Zhong *et al.*, 2015; Luo *et al.*, 2016).

5 Conclusions

Hybrid layers of the adhesive resins used in this study could be remineralized by placement in a BRM. However, this method cannot yet be used clinically. Rhodamine B uptake in conjunction with CLSM is a useful tool to quantify remineralization effects on hybrid layers. iBond hybrid layers showed the highest Rhodamine B uptake, followed by FluoroBond II and then Xeno-III-Bond, indicating variation in the quality of the hybrid layers following the use of different adhesives.

Compliance with ethics guidelines

Hui-ping LIN, Jun LIN, Juan LI, Jing-hong XU, and Christian MEHL declare that they have no conflict of interest.

All procedures followed were in accordance with the ethical standards of the responsible committee on human experimentation (institutional and national) and with the Helsinki Declaration of 1975, as revised in 2008 (5). Informed consent was obtained from all patients for being included in the study.

References

Baht, G.S., Hunter, G.K., Goldberg, H.A., 2008. Bone sialoprotein-collagen interaction promotes hydroxyapatite nucleation. *Matrix Biol.*, **27**(7):600-608. http://dx.doi.org/10.1016/j.matbio.2008.06.004

Cai, Y., Tang, R., 2008. Calcium phosphate nanoparticles in biomineralization and biomaterials. *J. Mater. Chem.*, **18**: 3775-3787. http://dx.doi.org/10.1039/B805407J

Carrilho, M.R., Tay, F.R., Pashley, D.H., *et al*., 2005. Mechanical stability of resin-dentin bond components. *Dent. Mater.*, **21**(3):232-241. http://dx.doi.org/10.1016/j.dental.2004.06.001

Carrilho, M.R., Geraldeli, S., Tay, F., *et al.*, 2007. In vivo preservation of the hybrid layer by chlorhexidine. *J. Dent. Res.*, **86**(6):529-533. http://dx.doi.org/10.1177/154405910708600608

Eanes, E., 2001. Amorphous calcium phosphate. *In*: Chow, L.C., Eanes, E.D. (Eds.), Octacalcium Phosphate. Monographs in Oral Science, Karger, Basel, Vol. 18, p.130-147. http://dx.doi.org/10.1159/000061652

Fontana, M., Li, Y., Dunipace, A.J., *et al.*, 1996. Measurement of enamel demineralization using microradiography and confocal microscopy. A correlation study. *Caries Res.*, **30**(5):317-325.

Gajjeraman, S., Narayanan, K., Hao, J., *et al*., 2007. Matrix macromolecules in hard tissues control the nucleation and hierarchical assembly of hydroxyapatite. *J. Biol. Chem.*, **282**(2):1193-1204. http://dx.doi.org/10.1074/jbc.M604732200

Glimcher, M., 2006. Bone: nature of the calcium phosphate crystals and cellular, structural, and physical chemical mechanisms in their formation. *Rev. Mineral. Geochem.*, **64**(1):223-282. http://dx.doi.org/10.2138/rmg.2006.64.8

Gu, L.S., Huffman, B.P., Arola, D.D., *et al.*, 2010. Changes in stiffness of resin-infiltrated demineralized dentin after remineralization by a bottom-up biomimetic approach. *Acta Biomater.*, **6**(4):1453-1461. http://dx.doi.org/10.1016/j.actbio.2009.10.052

Hashimoto, M., 2010. A review—micromorphological evidence of degradation in resin-dentin bonds and potential preventional solutions. *J. Biomed. Mater. Res. B Appl. Biomater.*, **92**(1):268-280. http://dx.doi.org/10.1002/jbm.b.31535

Hashimoto, M., Nakamura, K., Kaga, M., *et al*., 2008. Crystal growth by fluoridated adhesive resins. *Dent. Mater.*, **24**(4):457-463. http://dx.doi.org/10.1016/j.dental.2007.04.014

He, G., Gajjeraman, S., Schultz, D., *et al.*, 2005. Spatially and temporally controlled biomineralization is facilitated by interaction between self-assembled dentin matrix protein 1 and calcium phosphate nuclei in solution. *Biochemistry*, **44**(49):16140-16148. http://dx.doi.org/10.1021/bi0510451

Jardine, A.P., da Rosa, R.A., Santini, M.F., *et al.*, 2016. The effect of final irrigation on the penetrability of an epoxy resin-based sealer into dentinal tubules: a confocal microscopy study. *Clin. Oral Invest.*, **20**(1):117-123. http://dx.doi.org/10.1007/s00784-015-1474-8

Kim, J., Vaughn, R.M., Gu, L., *et al.*, 2010. Imperfect hybrid layers created by an aggressive one-step self-etch adhesive in primary dentin are amendable to biomimetic remineralization in vitro. *J. Biomed. Mater. Res. A*, **93**(4): 1225-1234. http://dx.doi.org/10.1002/jbm.a.32612

Kim, Y.K., Mai, S., Mazzoni, A., *et al.*, 2010a. Biomimetic remineralization as a progressive dehydration mechanism of collagen matrices—implications in the aging of resin-dentin bonds. *Acta Biomater.*, **6**(9):3729-3739. http://dx.doi.org/10.1016/j.actbio.2010.03.021

Kim, Y.K., Gu, L.S., Bryan, T.E., *et al.*, 2010b. Mineralisation of reconstituted collagen using polyvinylphosphonic acid/ polyacrylic acid templating matrix protein analogues in the presence of calcium, phosphate and hydroxyl ions. *Biomaterials*, **31**(25):6618-6627. http://dx.doi.org/10.1016/j.biomaterials.2010.04.060

Kinney, J.H., Habelitz, S., Marshall, S.J., *et al*., 2003. The importance of intrafibrillar mineralization of collagen on the mechanical properties of dentin. *J. Dent. Res.*, **82**(12): 957-961. http://dx.doi.org/10.1177/154405910308201204

Kokubo, T., Kushitani, H., Sakka, S., *et al*., 1990. Solutions able to reproduce in vivo surface-structure changes in bioactive glass-ceramic A-W. *J. Biomed. Mater. Res. A*, **24**(6):721-734. http://dx.doi.org/10.1002/jbm.820240607

Li, H., Burrow, M.F., Tyas, M.J., 2000. Nanoleakage patterns of four dentin bonding systems. *Dent. Mater.*, **16**(1):48-56. http://dx.doi.org/10.1016/S0109-5641(99)00085-8

Lin, J., Mehl, C., Yang, B., *et al*., 2010. Durability of four composite resin cements bonded to dentin under simulated pulpal pressure. *Dent. Mater.*, **26**(10):1001-1009. http://dx.doi.org/10.1016/j.dental.2010.06.004

Lin, J., Zheng, W.Y., Liu, P.R., *et al.*, 2014. Influence of casein phosphopeptide-amorphous calcium phosphate application, smear layer removal, and storage time on resin-dentin bonding. *J. Zhejiang Univ.-Sci. B (Biomed. & Biotechnol.)*, **15**(7):649-660. http://dx.doi.org/10.1631/jzus.B1300216

Liu, Y., Tjäderhane, L., Breschi, L., *et al.*, 2011. Limitations in bonding to dentin and experimental strategies to prevent bond degradation. *J. Dent. Res.*, **90**(8):953-968. http://dx.doi.org/10.1177/0022034510391799

Luo, X.J., Yang, H.Y., Niu, L.N., *et al.*, 2016. Translation of a solution-based biomineralization concept into a carrier-based delivery system via the use of expanded-pore mesoporous silica. *Acta Biomater.*, **31**(10):378-387. http://dx.doi.org/10.1016/j.actbio.2015.11.062

Mai, S., Kim, Y.K., Toledano, M., *et al.*, 2009. Phosphoric acid esters cannot replace polyvinylphosphonic acid as phosphoprotein analogs in biomimetic remineralization of resin-bonded dentin. *Dent. Mater.*, **25**(10):1230-1239. http://dx.doi.org/10.1016/j.dental.2009.05.001

Meyer, J.L., Weatherall, C.C., 1982. Amorphous to crystalline calcium phosphate phase transformation at elevated pH. *J. Colloid Interface Sci.*, **89**(1):257-267. http://dx.doi.org/10.1016/0021-9797(82)90139-4

Olszta, M.J., Odom, D.J., Douglas, E.P., *et al*., 2003. A new paradigm for biomineral formation: mineralization via an amorphous liquid-phase precursor. *Connect. Tissue Res.*, **44**(1):326-334. http://dx.doi.org/10.1080/03008200390181852

Pashley, D.H., Tay, F.R., Yiu, C., *et al*., 2004. Collagen degradation by host-derived enzymes during aging. *J. Dent. Res.*, **83**(3):216-221. http://dx.doi.org/10.1177/154405910408300306

Pashley, D.H., Tay, F.R., Carvalho, R.M., *et al.*, 2007. From dry bonding to water-wet bonding to ethanol-wet bonding. A review of the interactions between dentin matrix and solvated resins using a macromodel of the hybrid layer. *Am. J. Dent.*, **20**(1):7-20.

Pfarrer, A., Faller, R., Dusehner, H., 1996. Application of confocal laser scanning microscopy for studying remineralization and demineralization processes. *J. Dent. Res.*, **1**(75):543.

Sauro, S., Osorio, R., Watson, T.F., *et al*., 2015. Influence of phosphoproteins' biomimetic analogs on remineralization of mineral-depleted resin–dentin interfaces created with ion-releasing resin-based systems. *Dent. Mater.*, **31**(7): 759-777. http://dx.doi.org/10.1016/j.dental.2015.03.013

Sidhu, S.K., Watson, T.F., 1998. Interfacial characteristics of resin-modified glass-ionomer materials: a study on fluid permeability using confocal fluorescence microscopy. *J. Dent. Res.*, **77**(9):1749-1759. http://dx.doi.org/10.1177/00220345980770091101

Tay, F.R., Pashley, D.H., 2008. Guided tissue remineralisation of partially demineralised human dentine. *Biomaterials*, **29**(8):1127-1137. http://dx.doi.org/10.1016/j.biomaterials.2007.11.001

Tay, F.R., Pashley, D.H., 2009. Biomimetic remineralization of resin-bonded acid-etched dentin. *J. Dent. Res.*, **88**(8): 719-724. http://dx.doi.org/10.1177/0022034509341826

Tay, F.R., Pashley, D.H., Rueggeberg, F.A., *et al*., 2007. Calcium phosphate phase transformation produced by the interaction of the Portland cement component of white mineral trioxide aggregate with a phosphate-containing fluid. *J. Endod.*, **33**(11):1347-1351. http://dx.doi.org/10.1016/j.joen.2007.07.008

Tjaderhane, L., Larjava, H., Sorsa, T., *et al*., 1998. The activation and function of host matrix metalloproteinases in dentin matrix breakdown in caries lesions. *J. Dent. Res.*, **77**(8):1622-1629. http://dx.doi.org/10.1177/00220345980770081001

Toroian, D., Lim, J.E., Price, P.A., 2007. The size exclusion characteristics of type I collagen: implications for the role of noncollagenous bone constituents in mineralization. *J. Biol. Chem.*, **282**(31):22437-22447. http://dx.doi.org/10.1074/jbc.M700591200

Trebacz, H., Wojtowicz, K., 2005. Thermal stabilization of collagen molecules in bone tissue. *Int. J. Biol. Macromol.*, **37**(5):257-262. http://dx.doi.org/10.1016/j.ijbiomac.2005.04.007

van der Veen, M.H., Tsuda, H., Arends, J., *et al*., 1996. Evaluation of sodium fluorescein for quantitative diagnosis of root caries. *J. Dent. Res.*, **75**(1):588-593.

Wang, Y., Spencer, P., 2005. Interfacial chemistry of class II composite restoration: structure analysis. *J. Biomed. Mater. Res. A*, **75**(3):580-587. http://dx.doi.org/10.1002/jbm.a.30451

Watson, T.F., Cook, R.J., Festy, F., *et al*., 2008. Optical imaging techniques for dental biomaterials interfaces. *In*: Curtis, R.V., Watson, T.F. (Eds.), Dental Biomaterials: Imaging, Testing and Modelling. Woodhead Publishing, Cambridge, Chapter 2, p.37-57. http://dx.doi.org/10.1533/9781845694241.37

Xu, A.W., Ma, Y., Cölfen, H., 2007. Biomimetic mineralization. *J. Mater. Chem.*, **17**(5):415-449. http://dx.doi.org/10.1039/B611918M

Yang, B., Ludwig, K., Adelung, R., *et al*., 2006. Micro-tensile bond strength of three luting resins to human regional dentin. *Dent. Mater.*, **22**(1):45-56. http://dx.doi.org/10.1016/j.dental.2005.02.009

Zhang, S., 2003. Fabrication of novel biomaterials through molecular self-assembly. *Nat. Biotechnol.*, **21**(10):1171-1178. http://dx.doi.org/10.1038/nbt874

Zhong, B., Peng, C., Wang, G., *et al*., 2015. Contemporary research findings on dentine remineralization. *J. Tissue Eng. Regen. Med.*, **9**(9):1004-1016. http://dx.doi.org/10.1002/term.1814

中文概要

题　目：牙本质粘结混合层仿生再矿化的体外研究

目　的：探讨再矿化介质聚乙烯磷酸和聚丙烯酸对 3 种粘结剂（FluoroBond II、Xeno-III 和 iBond）和牙本质所形成的树脂-牙本质界面再矿化程度的影响。

创新点：（1）多数仿生再矿化研究集中于通过透射电子显微镜观察牙本质粘结剂界面的再矿化情况，鲜有采用激光共聚焦显微镜（CLSM）作为观察手段的。虽有研究应用 CLSM，但也仅是从定性的角度比较再矿化效应，没有定量分析比较，难以令人信服。而本项研究从定性和定量两方面分析对比。（2）本研究从当前牙本质粘结剂系统（共七代）常用的后四代中选择典型代表产品为研究对象，便于横向比较各类粘结剂。（3）本研究的定量结果除了比较同一时间实验组和对照组的矿化情况，还增加了纵向分析思路，进一步比较矿化程度随时间的变化以及不同牙本质粘结剂粘结界面的矿化情况。

方　法：将 96 颗健康前磨牙按照 FluoroBond II、Xeno-III 和 iBond 粘结剂随机分为 3 组，每颗牙均暴露表层牙本质。3 种粘结剂分别严格按照各自产品说明书处理牙本质表面，牙合面堆制 5 mm 厚的树脂。每颗牙沿牙合-龈向切成 0.9 mm 厚的薄片，获取中间两片样本用于矿化组和模拟组。矿化组采用含聚乙烯磷酸和聚丙烯酸的再矿化液浸泡；模拟组采用不含聚乙烯磷酸和聚丙烯酸的模拟体液浸泡。各组标本在储存 1、2、3 和 4 个月后，各取出 8 片，经苏丹明 B 荧光染料染色 24 h，冲洗，吹干，置 CLSM 下观察渗入混合层及粘结层的荧光情况，测量荧光面积、平均荧光量及总荧光量。所有数据统计方法采用方差分析（ANOVA）和 Tukey's HSD 检验分析。

结　论：本研究中聚丙烯酸和聚乙烯磷酸双仿生类似物分子对 FluoroBond II、Xeno-III 及 iBond 粘结剂均显示不同程度的再矿化效应，其中对 iBond 粘结剂再矿化效应最明显，FluoroBond II 粘结剂次之，Xeno-III 粘结剂再矿化效应较差，但能够起到抵制基底矿物继续丢失或阻止胶原降解的作用。CLSM 结合应用苏丹明 B 是量化混合层再矿化的一项有效手段。因此，上述双仿生类似物分子应用于口腔粘结剂修复材料促使混合层再矿化，具有良好的应用前景，值得进一步深入研究。

关键词：再矿化；牙本质；粘结树脂；仿生类似物；激光共聚焦显微镜；荧光